Lavalette *et al. Appl Adhes Sci (2017) 5:20*
https://doi.org/10.1186/s40563-017-0100-1

Applied Adhesion Science

RESEARCH Open Access

Comparative study of adhesive joint designs for composite trusses based on numerical models

N. P. Lavalette*, O. K. Bergsma, D. Zarouchas and R. Benedictus

*Correspondence:
n.p.lavalette@tudelft.nl
Faculty of Aerospace Engineering–Structural Integrity & Composites, Delft University of Technology, Kluyverweg, 2629HS Delft, The Netherlands

Abstract

In the context of lightweight structure design for the transportation and robotics industries, new types of composite structures are being developed, in the form of trusses made of fiber-reinforced polymer composite members of small diameter (a few millimeters thick at most). Some concepts of wound trusses can be found in the literature, but in more general cases, for which a predefined wound truss shape is not usable, individual truss members must be joined together. The axial strength of the composite members allow them to carry a high load, and the joints between those members should be strong enough to carry this load as well. With the objective of developing an efficient joint design for an application in thin composite trusses (member thickness ranging from 0.5 to 5 mm), finite element models of several adhesive joint designs were built, and their strengths were compared. The comparison was made using the same joint configuration (number of members, member cross-sectional area, joint dimensions) and loading conditions. Adhesive failure was considered in this study, and the strength of each design was determined from the value of the peak maximum principal strain in the adhesive layer, as this failure criterion is suitable for the toughened adhesive material used in the models. A trade-off between the strength, weight and manufacturability of each joint design was made in order to conclude on their overall performance. Results suggested that, among the joint designs modelled, round-based composite rods inserted in a tubular metallic piece are the most efficient in terms of strength-to-weight ratio.

Keywords: Bonded joints, Carbon fiber reinforced polymer, Numerical study, Finite element method, Trusses

Background

In transportation engineering, and particularly in aerospace and automotive engineering, reducing the weight of structures has for decades been one of the primary concerns. A structure achieving the same mechanical properties, while being lighter than the currently used one, leads to a reduced fuel consumption, serving economics and environmental impact. Thanks to their low density and good mechanical properties, carbon fiber composite materials are used more and more often in those industries, especially since they are getting more affordable and easier to manufacture. The present paper stands in this context, aiming at making use of the very high tensile strength of carbon

fiber reinforced polymers to design lightweight structures for the industries looking for weight reduction.

In order to obtain structures that are more efficient, either lighter or stronger or both, optimization methods focused on trusses have been developed over the years, starting with the precursory work of Michell [1], and the later introduction of the ground structure method by Dorn et al. [2]. Although simple algorithms, such as the ones provided by Zegard and Paulino for two-dimensional [3] and three-dimensional [4] trusses, can already give solutions to optimization problems, work has been done to develop methods that include more variables and perform better. For example, Gao et al. [5] used the directions of the principal stresses in the design domain to guide the algorithm towards more efficient solutions, Zhang et al. [6] reduced the computational costs by dividing the design domain in several elements and carrying the optimization on each element, and He and Gilbert [7] included variables aimed at making the final solutions realistic and geometrically doable. A whole research branch in truss optimization is also dedicated to the use of metaheuristic methods, with for example the use of genetic algorithms by Rajan [8] and Deb and Gulati [9], a multi-population evolutionary method by Wu and Tseng [10], or an harmony search algorithm by Lee and Geem [11]. But despite the considerable improvements made in truss optimization over the years, those methods do not consider the strength of the joints of the structure as an optimization variable. Typically, the designers focus on the topology of the structural members and their optimization, then they investigate the joints. In the case of small scale trusses made of pultruded carbon fiber members, for which adhesive bonding is the most likely candidate for the joints and considering the fact that adhesives have a much lower strength than the members, including the strength of the joints as a variable in the design optimization process is necessary.

The manufacturing of complex composite truss structures has been a subject of interest in recent years, due to the advancements made in manufacturing processes. Woods et al. [12] developed a tube-like truss structure made of carbon fibers wound and cured around a "skeleton" of pultruded chord members, also made of carbon fiber reinforced polymer. Weaver and Jensen [13] developed and commercialized a composite lattice carbon fiber structure concept called IsoTruss that was manufactured using a braiding machine. Those examples use a manufacturing process for which it is not necessary to produce individual joints, but the results are generic geometries, limiting the range of applications for the trusses made with these concepts. In order to be able to realize trusses of any shape, and that can therefore be theoretically developed for any kind of application, either two- or three-dimensional, the joints of the truss must be produced separately and assembled with the truss members.

When an efficient joint design is selected for composite truss structures, it can then be further optimized so that it is able to carry the load efficiently between the truss members, while adding as little weight as possible to the structure. It can also be used within the truss optimization algorithm, in order for the optimizer to use the strength of the joints into account when calculating the most efficient structure. This paper proposes to model and analyze several joint design concepts, in order to compare their performances in terms of strength and weight and select the one(s) that perform the best, for an application in composite trusses and truss optimization.

Selected concepts

The proposed solution consists of designing joints that make use of the load transfer capabilities of the adhesive in shear. Previous experimental and numerical work [14] have found that directly joining the members together through adhesive bonding, as shown on Fig. 1, produces a joint that has a low efficiency. Instead, it is proposed to include at the center of the joint an intermediary piece overlapping the members. The members are adhesively bonded at the overlap with the central joint piece, and the joints are therefore expected to have a better efficiency by transferring the load to this intermediary piece instead of to each other directly.

Three joint designs will be analyzed in this study, and are presented in Fig. 2. In order to study the influence of the cross-sectional shape of the members, two of the joint designs have two variants each, one using square-based members and one using round-based members, making it five joint designs in total:

- The first joint design, called J1 in this paper and presented in Fig. 2a, is inspired by the gusset plates present in civil engineering trusses, and consists of having square based members adhesively bonded between two plates, similarly to a double-lap joint. The plates have the advantage of being easily manufactured, but the main issue with this type of design is that it can only be applied to two-dimensional trusses. To be used for three-dimensional trusses, elaborate shapes would need to be produced, and the advantage stated above is lost. This joint design does not have a round-based variant, since round-based members cannot be bonded to plates using a constant adhesive thickness.
- The second group of joint designs, called J2s and J2r for the variants using square-based and round-based members respectively, and presented in Fig. 2b, consists of inserting a plate in the extremities of the members, so that the members are adhesively bonded to both sides of the plate. It is inspired by the work done by Vallée et al. [15] on adhesive joints in timber trusses, in which a similar joint consisting of a plate around which the members are adhesively bonded was studied. Similarly to the joint design J1, these joint designs can however only be used for two-dimensional trusses.
- The third group of joint designs, called J3s and J3r for the variants using square-based and round-based members respectively, and presented in Fig. 2c, consists of having a central joint piece that completely surrounds the members and is adhesively bonded to them, similarly to the lugged steel frame construction used to build bicycle

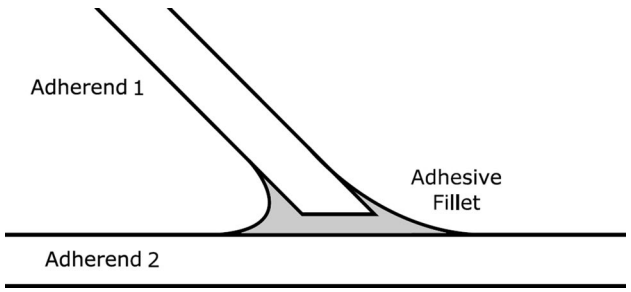

Fig. 1 CFRP truss members joined together through adhesive bonding [14]

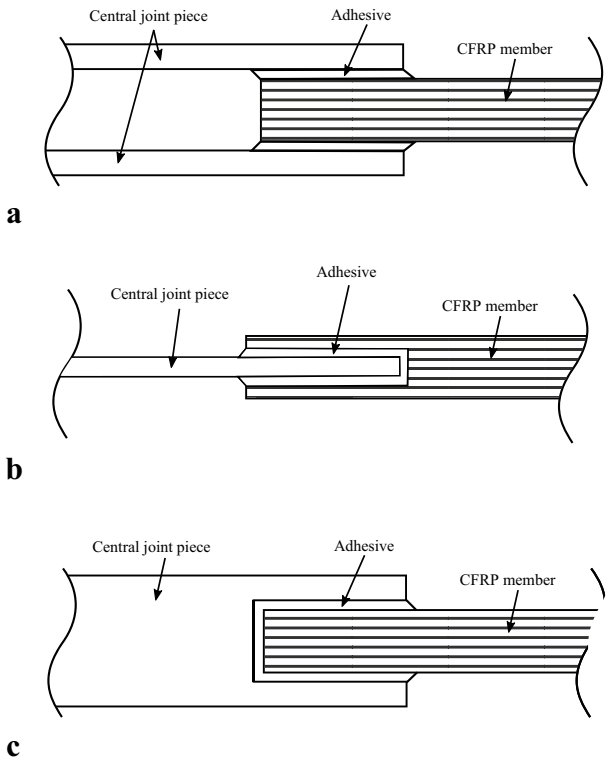

Fig. 2 Joint concepts analyzed in this study. **a** J1, **b** J2s and J2r, **c** J3s and J3r

frames. The main advantage of these joint designs is that they can be used for three-dimensional trusses, since there is no restriction due to the flat nature of the central joint piece as there is in the two previous joint designs. Furthermore, if the material selected for the central joint is isotropic, it could mitigate the issues related to out-of-plane stresses that can arise in three-dimensional structures and be problematic for fiber-reinforced components. It is expected that these joint designs are stronger than the J1 and J2 designs, due to the adhesive overlap completely surrounding the members.

Methods

Ever since adhesively bonded joints grew in popularity among engineering applications, closed-form analytical models have been introduced. Many different models are available in the literature, each suitable for different joint configurations and with a different level of complexity, from the first classical models of Volkersen [16] and Goland and Reissner [17], to more advanced general models suitable for modelling any type of joint configuration, such as the model proposed by Bigwood and Crocombe [18]. Despite their simplicity, closed-form models generally show some important limitations. The shear- and peel stress distribution is assumed uniform over the adhesive thickness. This simplification implies that adherend–adhesive interface stresses, which play a significant role in failure analysis, are not considered. Another limitation of those models is that complex joint shapes and local end geometry, such as an adhesive fillet, are not included.

Due to those limitations, the use of a closed-form model to determine the stress distribution in the joint designs proposed in this study would prove hard to implement and of limited interest. Therefore, strength predictions for the different joint designs are made by the numerical analysis of finite elements models built for each one of them. Three-dimensional finite elements models are built for this purpose, Goncalves et al. [19] having observed the three-dimensional nature of the stresses occurring in a joint, showing that two-dimensional models should be taken with care.

Geometry and material properties of the numerical models

In order to be able to compare the results obtained from the analyses of the different finite elements models, a common set of rules need to be followed while building them. Otherwise, the differences in strength could be attributed to differences in the joint layout instead of the differences in design only, which are the purpose of this study. The effects of the dimensions of the joint (such as the adhesive layer thickness and the overlap length) on its strength are well documented in the literature. Results show that the joint strength decreases with the increase of the adhesive layer thickness [20, 21], and that the joint strength is linearly proportional to the joint width [22]. Furthermore, considering that a ductile adhesive is used, the joint strength increases almost proportionally with the joint length because ductile adhesives deform plastically and make use of the whole overlap [23], contrary to brittle adhesives which cannot accommodate peak stresses at the ends of the overlap [24]. The effects of varying the joint dimensions are not studied in the present paper. Instead, one set of dimensions is selected and applied to all joint designs, and the effects of the design differences is studied. This set of dimensions is selected with regards to the scale of the envisioned applications, with trusses in the meter-range containing members that are a few millimeters thick. It is to be noted that the dimensions described further are chosen semi-arbitrarily, in the sense that they are realistic but not optimized for the best joint performance. The testing, analysis and optimization of the joint design selected as the result of this study will be the subject of a later publication.

In all the designs, the joint has the same layout, as shown in Fig. 3. The joint is considered as two-dimensional, in the sense that the truss members joining are all located in the same plane. The members are separated by an angle of 120°, allowing an additional symmetry in the numerical models (shown as dotted lines in Fig. 3) and therefore a lower computational cost. The members are 25 mm long, the overlap between the members and the central joint piece is 5 mm, and the distance between the loading edge of the central joint piece and its center is 7 mm. The cross-sectional area of the members is taken as 9 mm^2, the dimensions of the different cross-sectional shapes being chosen accordingly to obtain this area. The adhesive layer is 0.2 mm thick, and a small triangular adhesive fillet is present at the ends of the overlap, with the same thickness as the adhesive layer. The minimum thickness of the central joint piece is 0.5 mm.

Following the same logic, the material properties of the members, central joint piece and adhesive are the same across the numerical models. Similarly to the geometry parameters of the joints, the mechanical properties of the materials used for the joints and members are not variable in this study, therefore their choice is of limited importance and will not affect the comparison, as long as they are consistent across the

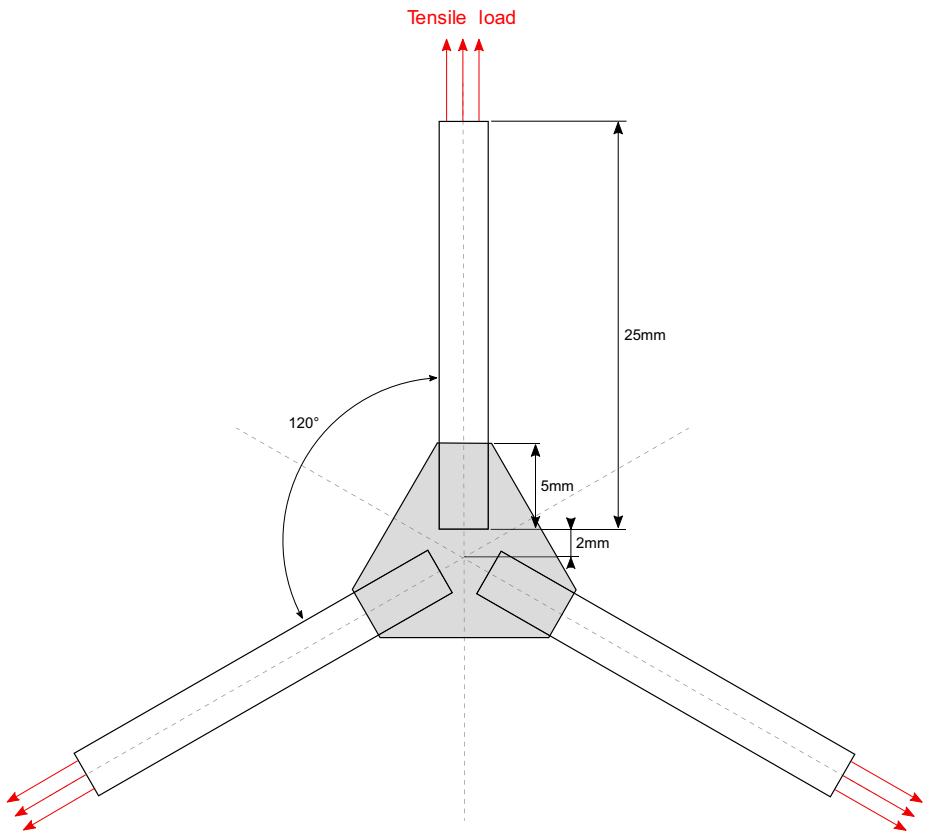

Fig. 3 Layout of the joint design J1, applied similarly to the other joint designs

numerical models. Nevertheless, it is preferable to model materials that are likely to be used in practice, and to accurately know their mechanical properties.

The members are unidirectional carbon-fiber-reinforced polymer rods. The composite material considered for the members is composed of typical intermediate modulus carbon fibers, Zoltek PX35 [25], combined with the Epikote MGS LR285 resin [26]. The material properties are taken from the datasheets of both constituents and presented in Table 1. The Poisson's ratio of both constituents are not present in the datasheets, but typical values for these types of materials are used. Based on the properties of the two constituents and the law of mixtures, the mechanical properties of the composite material, in the form of engineering constants, are calculated and presented in Table 2.

Table 1 Mechanical properties of Zoltek PX35 [25] carbon fibers and Epikote MGS LR285 resin [26]

Material property	Zoltek PX35 fibers	Epikote MGS LR285 resin
Young's modulus (GPa), E	242	3.15 ± 0.15
Poisson's ratio, v	0.20	0.33
Shear modulus (GPa), G	10.08	1.184

Table 2 Engineering constraints of the carbon fiber composite

E_{11} (MPa)	E_{22} (MPa)	E_{33} (MPa)	ν_{12}	ν_{13}	ν_{23}	G_{12} (MPa)	G_{13} (MPa)	G_{23} (MPa)
146,460	7724	7724	0.252	0.252	0.237	2517	2517	3121

The materials considered for the adhesive layer and the central joint piece are both isotropic materials. The material used for the adhesive layer in the numerical models is a rubber-toughened epoxy adhesive, Araldite 2015 [27]. The mechanical properties of this adhesive were determined in a study by Campilho et al. [28], along with another brittle adhesive of the same brand. The choice of a rubber-toughened ductile adhesive instead of a brittle one is based on the ductile adhesives' increased toughness due to particle cavitation, which increases their strength and makes them a preferred choice for aerospace applications [29]. The mechanical properties determined by Campilho et al. [28] are presented in Table 3 and used to build a bilinear material model (Fig. 4) to be implemented in the numerical models. The material taken for the central joint piece is an aluminum alloy common in aerospace industry, Aluminum 7075-T6 [30]. This study will not consider the eventual plastic deformation of the central joint piece, therefore only its linear elastic material properties will be implemented in the numerical models (Table 4).

Table 3 Mechanical properties of Araldite 2015 [27] as determined by Campilho et al. [28]

Property	Araldite 2015
Young's modulus (GPa)	1.85 ± 0.21
Poisson's ratio	0.33
Tensile yield strength (MPa)	12.63 ± 0.61
Tensile yield strain (%)	0.06 ± 0.05
Tensile failure stress (MPa)	21.63 ± 1.61
Tensile failure strain (%)	4.77 ± 0.15
Shear modulus (GPa)	0.56 ± 0.21
Shear yield stress (MPa)	14.6 ± 1.3
Shear failure stress (MPa)	17.9 ± 1.8
Shear failure strain (%)	43.9 ± 3.4
Density (g/cm^3)	1.4

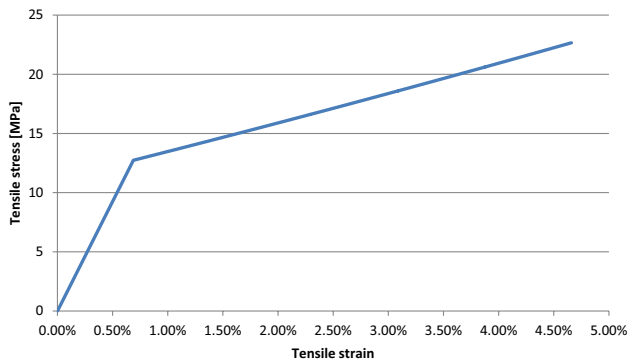

Fig. 4 Bilinear material model of Araldite 2015 [27] based on the mechanical properties determined by Campilho et al. [28]

Table 4 Mechanical properties of Aluminum 7075-T6 [30]

Property	Aluminum 7075-T6
Young's modulus (GPa)	71.7
Poisson's ratio	0.33

Numerical models

The software ABAQUS was used to perform the numerical analyses for this study. In order to ensure the robustness of the numerical models, a convergence study has been performed on the joint design J1. The resulting mesh refinement is shown on Fig. 5. The mesh size is refined close to the edges of the adhesive layer, as well as close to both adhesive-adherend interfaces. Close to the ends of the overlap, the adherends have a notably smaller mesh size than the more central regions, which was shown by Diaz et al. [31] to give better quality results, due to the gradient of stresses and strains making these locations mesh-sensitive. The size of the elements in the mesh-sensitive regions is 0.05 mm, while the elements away from the more mesh-sensitive regions are bigger: 0.1 mm along the width (X-direction) and thickness (Z-direction), 0.4 mm along the length (Y-direction). The adhesive layer features a small triangular fillet and the number of elements in the adhesive layer thickness is 4. The elements used for the adhesive and adherends are quadratic 20-nodes reduced integration hexahedral elements (called C3D20R in ABAQUS [32]). The same mesh refinement and elements were used on the other models, as best as possible considering their slightly differing geometries.

The material properties used for the adherends and adhesive are the ones presented in the previous section. Plasticity of the adhesive is considered, while for the adherends only elasticity is considered. Both the adhesive and the central joint piece are modelled as isotropic materials, whereas the composite member is modelled as a transversely isotropic material, its longitudinal direction being defined as the member's length direction.

The model represents 1/12th of the actual joint layout, thanks to the symmetries presented on Fig. 3. The boundary conditions corresponding to these symmetries are applied on the model as presented in Fig. 6. A tensile load is applied at the end of the

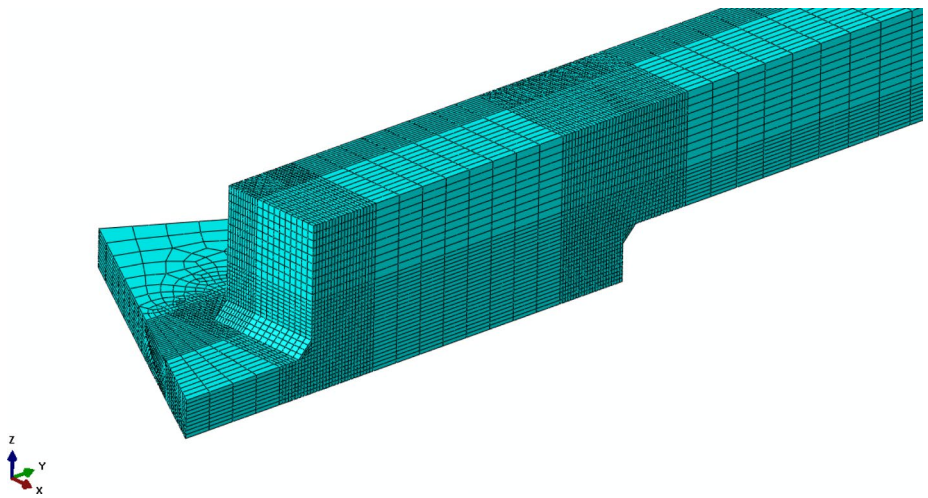

Fig. 5 Mesh refinement for the "double gusset" joint design (J1)

composite member, as represented on Fig. 3. The value of the applied load varies with each joint design analyzed, so that the load is high enough for the joint to reach failure.

Failure criterion

Traditionally in structural engineering, the efficiency of a joint is characterized as the ratio of the load that the joint can support before failure, over the load that the members can support before failure. Ideally, joints should have an efficiency greater than 100%, so that under an excessive load, the members fail before the joints, therefore minimizing the loss of structural integrity. In this study, only cohesive failure within the adhesive is considered as a failure of the joint. Other types of failure, such as adhesive failure or failure of either the composite members or central joint piece are not considered.

In order to assess failure within the adhesive, a failure criterion is needed. The suitability of different failure criteria for adhesives in single lap joints was studied by Harris and Adams [33], with the conclusion that for toughened ductile adhesive like the one used in the present study, the maximum principal strain is the best suited criterion. Further work carried out by Broughton et al. [22] also showed that strain-based failure criteria give more accurate results than stress-based failure criteria for adhesively bonded joints. Additionally, this work showed that a maximum principal strain criterion was better suited to scarf joints, whereas a peak shear strain criterion was better suited to lap joints. The models analyzed in this study have the characteristics of lap joints, thus the peak shear strain is chosen as failure criterion.

For each of the five joint design models, a non-linear analysis is performed, which includes the plasticity of the adhesive, using the bilinear model presented in Fig. 4, as well as geometric non-linearities. Since the joint designs analyzed in this study are similar to double-lap joints, it is assumed that the adherends are not subject to excessive deformation. Therefore adherend elasticity is assumed in the numerical models. Two types of results are extracted from each analysis: from the linear elastic part and from the non-linear part. The linear elastic part of the analyses is used to compare, for the

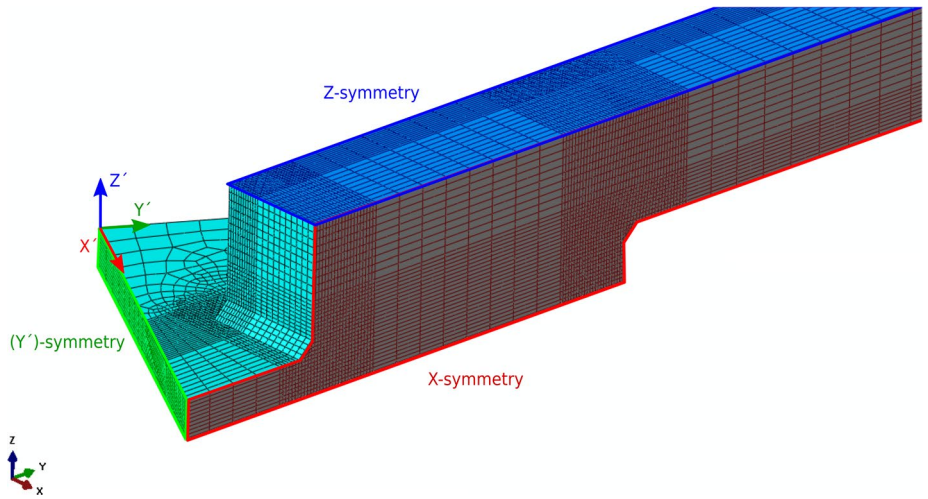

Fig. 6 Boundary conditions applied on the numerical models

same load, the value of the failure criterion within the adhesive for the different joint designs, with the idea that lower values of the failure criterion imply that a higher load is necessary for the adhesive to reach its yield point (and subsequently its failure point), meaning that the joint design considered is performing better. The non-linear part of the analyses is used to compare the loads at which the adhesive reaches its failure point, characterized by the peak shear strain reaching the shear failure strain of the adhesive (see the material properties in Table 3). For ductile adhesives which, contrary to brittle adhesives, allow the stresses to be redistributed along the overlap length as the material deforms plastically, the joint strength can be predicted more accurately by modeling the complete failure of the adhesive than taking the load at first failure. However, Campilho et al. [34, 35] found that for very short overlaps (corresponding to the overlap length used in this study) the shear stresses are nearly constant over the overlap length, resulting in the failure that depends almost exclusively on the adhesive strength. As a result, for very short overlaps, the higher fracture toughness of ductile adhesives becomes irrelevant, and they behave more like brittle adhesives. It is therefore assumed that the load at first failure of the adhesive is a good enough strength prediction for this comparative study. For a more accurate representation of the actual performance of the joints, experimental tests would be necessary to determine the validity of the failure criterion.

The non-linear behavior of the joint cannot be approximated with accuracy by a linear model. Nonetheless, comparing the linear behavior of the joints designs might already be an indication of their respective performance. Comparing both types of results aims at observing whether a linear elastic model can reach conclusions that are close to those obtained with a non-linear model, for a much lower computational cost.

Results

The results of both the linear elastic and non-linear analyses are presented in this section. Since the finite element software computes the stress and strain values at the integration points (Gauss points) of the elements, for all models and analyses the values of the shear strain for the failure criterion are taken at integration points to avoid interpolation inaccuracies from the integration points to the nodes [33]. Therefore, for the evaluation of the peak shear strain in the adhesive layer, the value is taken from the Gauss point closest to the peak shear strain displayed from the nodes, as it is assumed to have the peak value of the integration points of the adhesive layer.

It must be noted that in all joint designs, except J1, a part of the adhesive layer orthogonal to the loading direction was modelled (on the loading edge side for J2s and J2r, on the free edge side for J3s and J3r). These regions were modelled for convenience, as it was easier to model an adhesive layer than to create contact interactions between the member and the central joint piece. In practice, having adhesive in these regions should be avoided as much as possible, because it would be loaded in tension and fail at a lower load than the regions of the adhesive layer loaded in shear, thereby initiating cracks that could propagate through the "shear regions" and cause the joint to fail prematurely (as opposed to having adhesive loaded in shear only). As a result, the extraction of values from both the linear elastic and non-linear analyses do not take these regions into account.

Linear elastic analysis

The results of the linear elastic analyses are presented in Table 5, in the form of the peak shear strain in the adhesive layer. The location of the peak shear strain for each model is displayed in Fig. 7. They correspond to the points where the adhesive will yield first. Figures 8 and 9 display the shear stress and peel stress distributions, respectively. Those stress values are taken along a path along the middle length of the adhesive layer, going from the free edge to the loading edge. They do not serve as failure criteria for the study, but allow to have a better visual representation of the stress distribution in the adhesive layer of the different joint designs.

Non-linear analysis

The results of the non-linear analyses are presented in Table 6, in the form of the failure load, i.e. the first load at which an element from the adhesive layer reaches the shear failure strain value of the adhesive material (Table 6). The location of the peak shear strain at failure for each model is displayed in Fig. 10. These locations are important, since they

Table 5 Peak shear strain values in the adhesive layer for the different joint designs (linear elastic analysis)

Model	J1	J2s	J2r	J3s	J3r
Peak shear strain (%)	0.0866	0.0870	0.0880	0.0240	0.0236

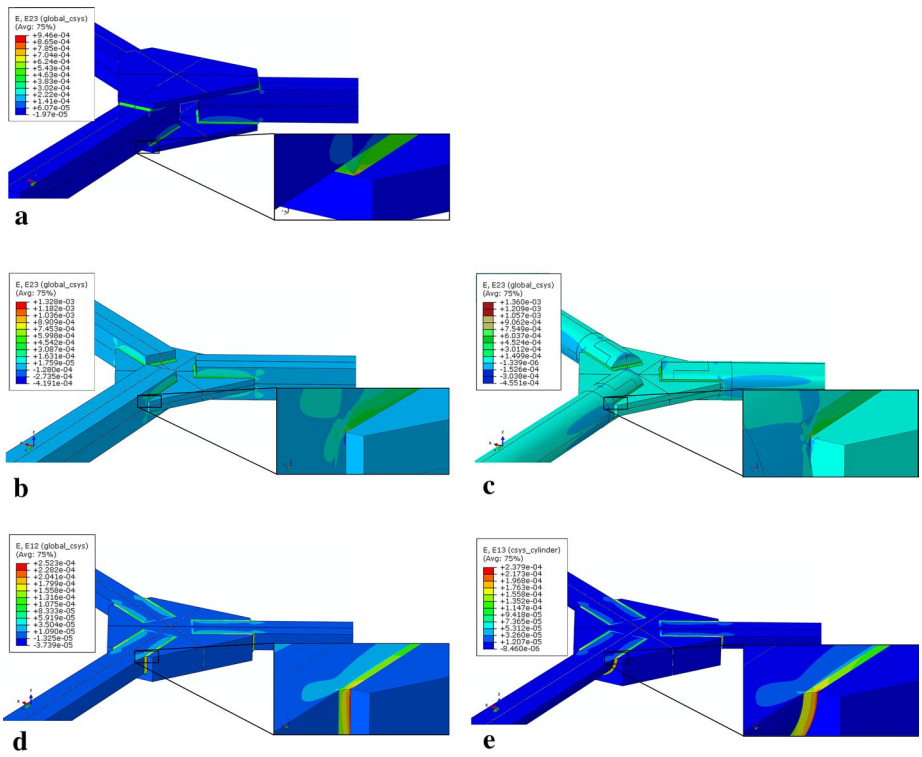

Fig. 7 Location of the peak shear strain in the adhesive layer for the different joint designs (linear elastic analysis). **a** J1, **b** J2s, **c** J2r, **d** J3s, **e** J3r

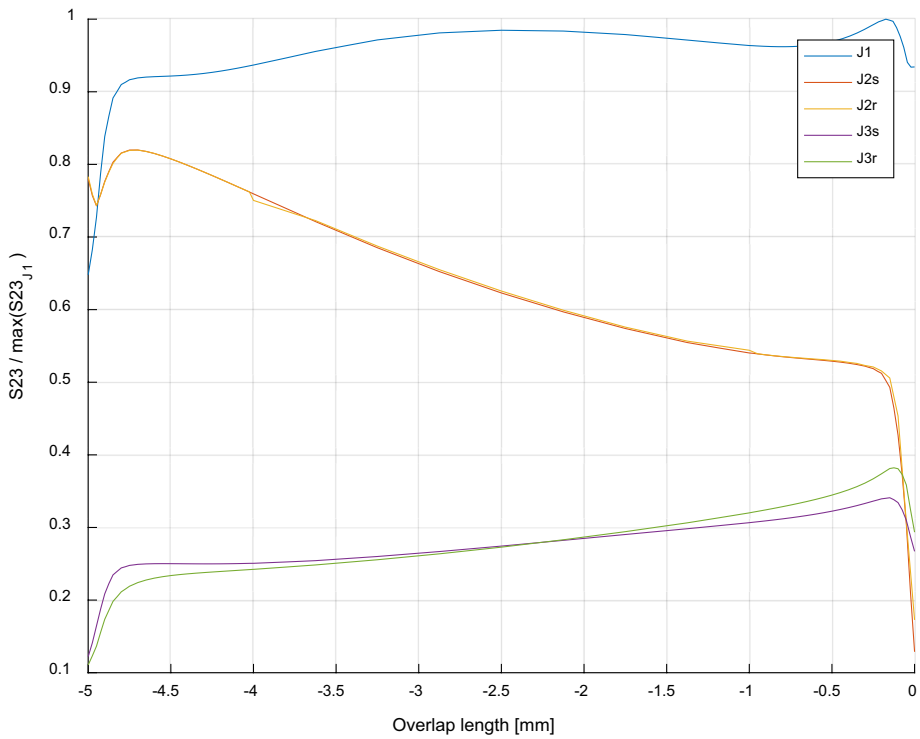

Fig. 8 Shear stresses distribution in the middle of the adhesive layer along the overlap length (on the X-symmetry plane) for the different joint designs

are assumed to correspond to the points where the adhesive will fail first, and therefore must be the primary target for further studies aimed at improving the first failure load of a specific joint design. It is important to note that the locations displayed here may be caused by singularity issues in the model, and that they should be taken as assumptions of failure points until further experiments validate or invalidate them.

Discussion

Linear elastic vs. non-linear analyses

Based on the results from both linear elastic and non-linear analyses, several conclusions can be made regarding the performance of the different joint designs. In order to compare the results from the linear elastic analyses (Table 5) with the results from the non-linear analyses (Table 6), the values of the peak shear strain obtained from the linear elastic analyses are inverted. This way, the decrease in the peak shear strain (characterizing an increase in the joint performance) can be more easily compared with increase in the failure load from the non-linear analyses. The results displayed in both Tables 5 and 6 are normalized and summed up in Fig. 11.

From the results of the linear elastic analyses, it appears that the joints designs J3s and J3r show a much better performance than the joint designs J1, J2s and J2r, with an increase in performance (with respect to J1) of 261 and 267% respectively for J3s and J3r, against a slight decrease of performance (with respect to J1) of 0.5 and 1.5% respectively for J2s and J2r. This suggests that the family of joint designs consisting of a full central

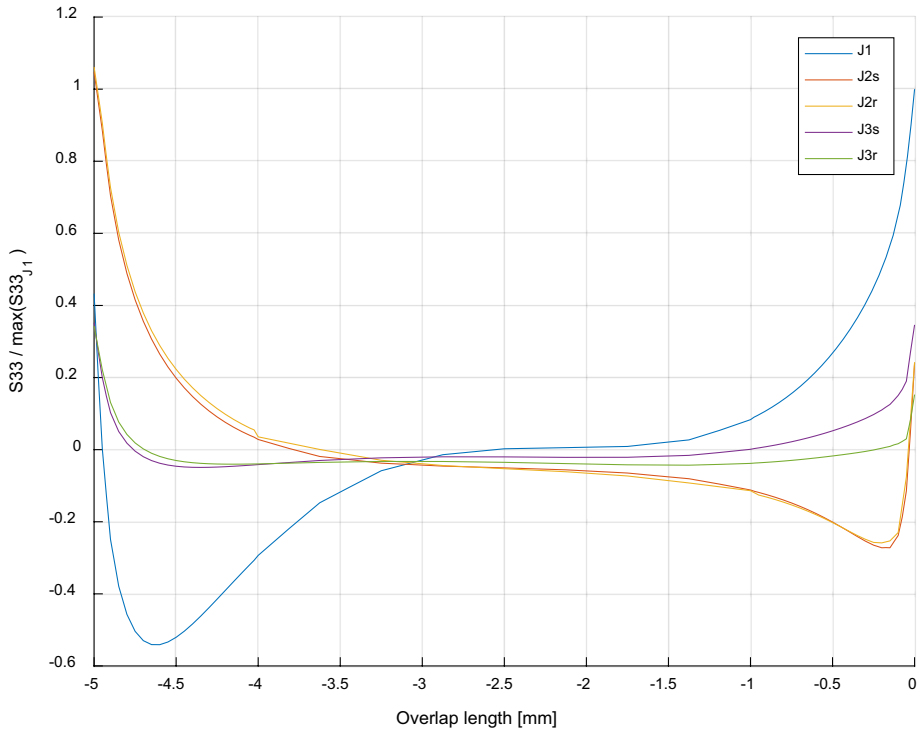

Fig. 9 Peel stresses distribution in the middle of the adhesive layer along the overlap length (on the X-symmetry plane) for the different joint designs

Table 6 Failure loads for the different joint designs (non-linear analysis)

Model	J1	J2s	J2r	J3s	J3r
Failure load (MPa)	43.77	75.82	78.29	231.6	227.25

joint piece that completely surrounds the members offer a much greater performance than the family of joint designs consisting of one or several plates. Those results were to be expected since the joint designs that completely surround the member have a larger surface of contact between the member, adhesive and central joint piece than the joints designs using one or several plates, this increase in adhesive surface resulting in lower stress concentrations within the adhesive and therefore an increased joint performance. Furthermore, those results show very small differences between the performances of the square-based and round-based versions of each design, suggesting that the choice of the shape of the member's cross section between square and round does not have a significant impact on the joint performance. The shear stress and peel stress distributions in the adhesive layer, displayed in Figs. 8 and 9, confirm the conclusion made above, by showing stresses that are significantly lower in the adhesive layers of joints J3s and J3r than those of joints J1, J2s and J2r, as well as showing very small differences between stress distributions of the square-based and round-based version of each joint design.

The results from the non-linear analyses lead to similar conclusions as the ones from the linear elastic analyses, with the exception that they suggest a better performance for

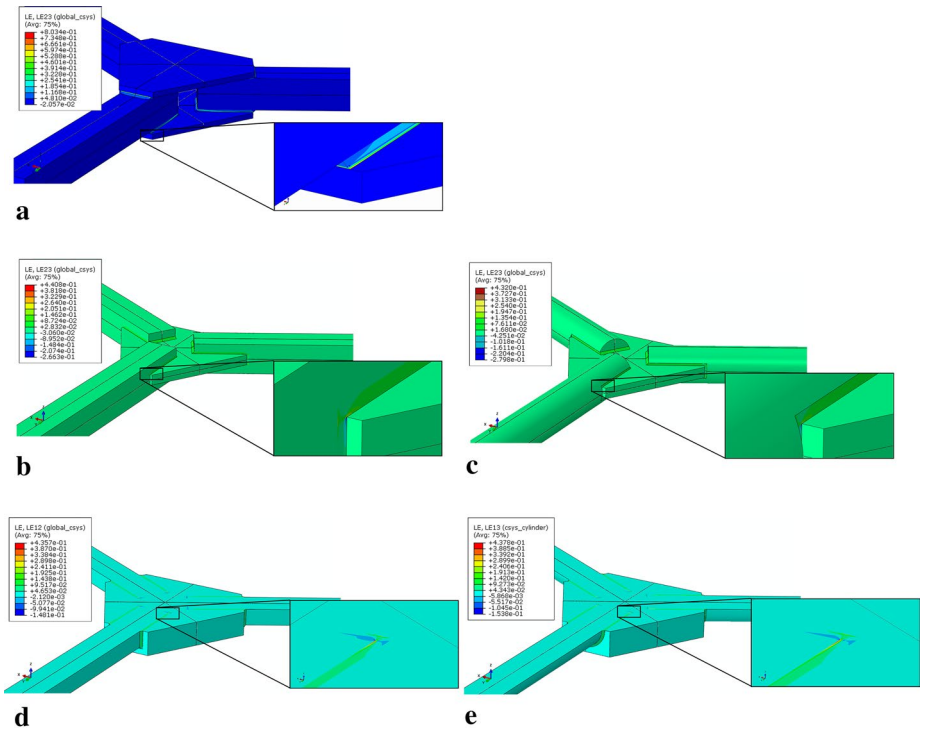

Fig. 10 Location of the peak shear strain at failure in the adhesive layer for the different joint designs (non-linear analysis). **a** J1, **b** J2s, **c** J2r, **d** J3s, **e** J3r

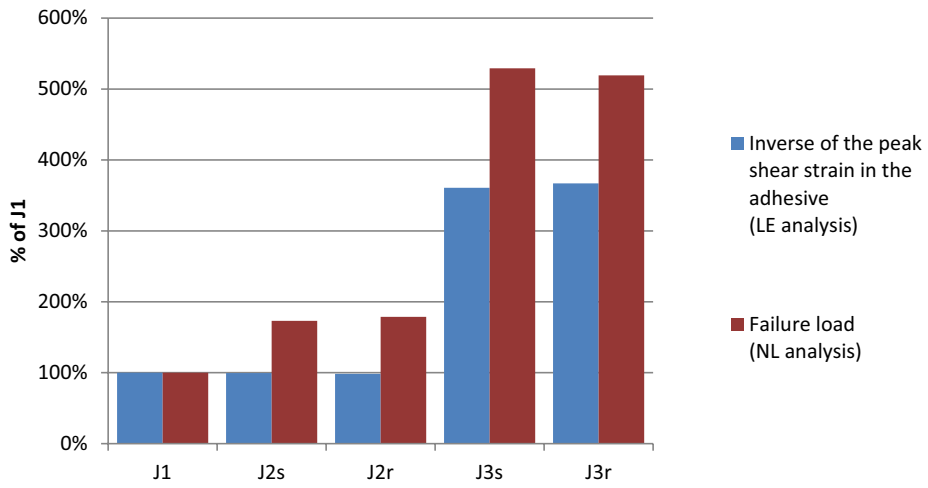

Fig. 11 Comparison of the performances of the different joint designs, as determined by the linear elastic and non-linear analyses

all joint designs compared to the linear elastic results. The joint designs J2s and J2r show an increase in performance (with respect to J1) of 73 and 79% respectively, whereas the linear elastic analyses showed a slight decrease of 0.5 and 1.5% respectively. The joint designs J3s and J3r show an increase in performance (with respect to J1) of 429 and 419% respectively, whereas the increase was of 261 and 267% respectively with the linear

elastic results. Similarly to the linear elastic analyses, very little differences are seen between the square-based and round-based version of each design. The non-linear models are more representative of the actual behavior and performances of the different joint designs, said performance being measured from the failure point rather than the yield point of the adhesive for the linear elastic models. The advantage of using the linear elastic model for predicting the performance of each joint design is that the computational cost is a lot lower. However, the discrepancies displayed on Fig. 11 between the results of both types of analyses suggest that the results from the linear elastic models are not reliable enough, since they cannot approach closely enough the results from the non-linear models.

Another difference between the results of the linear elastic and non-linear analyses can be seen on the Figs. 7 and 10, displaying the location of the peak shear strain in the adhesive layer after the linear elastic and non-linear analyses respectively. It must be noted that the location of the peak shear strain has a different meaning in each type of analysis. Whereas in the linear elastic analyses it represents the point of first yield of the adhesive layer, in the non-linear analyses it represents the point of first failure of the adhesive layer. Comparing these locations in both types of analyses show that for the joint designs consisting of one or several plates, J1, J2s and J2r, the point of first yield (Fig. 7a–c respectively) corresponds to the point of first failure (Fig. 10a–c respectively), and is located at the corners of the loading edge of the adhesive overlap. For the joint designs consisting in a central joint piece completely surrounding the member, J3s and J3r, the point of first yield (Fig. 7d, e respectively) is located on the loading edge of the adhesive layer, whereas the point of first failure (Fig. 10d, e respectively) is located on the "free edge" of the adhesive layer, i.e. the opposite side from the loading edge.

Performance vs. weight

As stated in the introduction, in many applications joints should not only be performant to ensure the integrity of a truss, but also be light weighted. In structural design, a balance must be found between performance and weight, as a more performant structure will most likely also be heavier and therefore may not fulfil the product requirements anymore. It is therefore important to compare the increase in performance of the different joint designs modelled in this study with their increase in weight. For all the models, the members have the same cross-sectional area and the same length, and the change of adhesive volume between the designs is negligible. Therefore, only the weights (or volumes, as it is equivalent) of the central joint piece of each joint design are used for this comparison, presented in Table 7. The increase in weight with respect to J1 is compared to the increase in performance resulting from the linear elastic and non-linear analyses in Figs. 12 and 13 respectively.

From the results of the linear elastic analyses, it appears that the increase in performance of each design does not always match the increase in weight of the joint piece volume. While there is no significant change in the performance and weight of the joint designs J2s and J2r (with respect to J1), the other joint designs show that the increase in performance is not proportional to the increase in weight, suggesting than some designs are more (or less) efficient than others. The increase in performance is higher than the increase in weight (with respect to J1) for the joint designs J3s and J3r. The joint designs

Table 7 Volume of the central joint piece for the different joint designs

Model	J1	J2s	J2r	J3s	J3r
Volume of the central joint piece (mm^3)	113.4	113.4	118.8	324	343.8

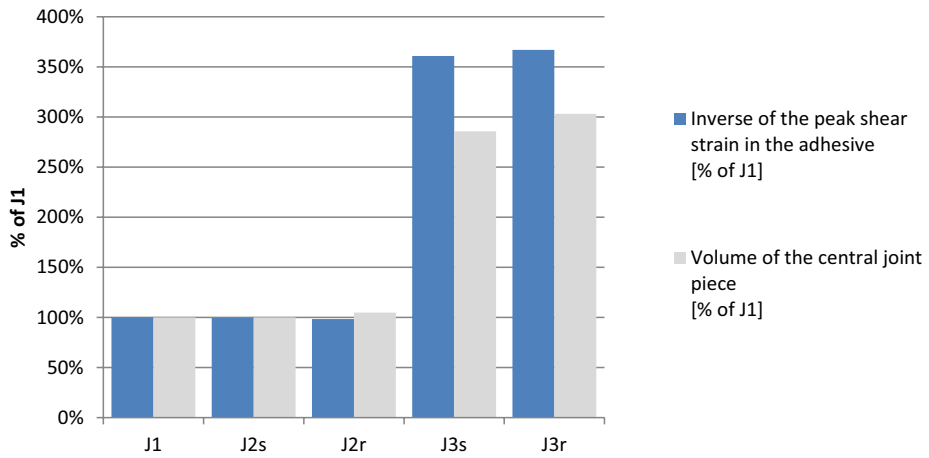

Fig. 12 Comparison of the volume increase with the performance increase (linear elastic analyses)

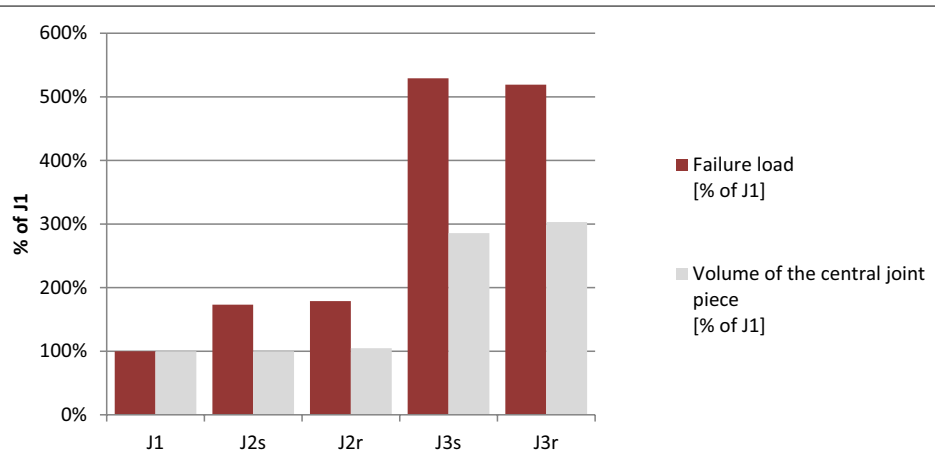

Fig. 13 Comparison of the volume increase with the performance increase (non-linear analyses)

J3s and J3r showing approximately the same performance and the same weight (although both are lightly higher for J3r), the results from the linear elastic analyses suggest that both designs can be applied in trusses with equal performances.

The results from the non-linear analyses confirm the conclusion made above, stating that the increase in joint performance is not proportional to the increase in weight. However, they suggest a different conclusion about the choice of square-based members over round-based members. Comparing the joint designs J3s and J3r, J3s shows a slightly lower weight, with an increase in weight of 186% (with respect to J1) for J3s against 203%

for J3r, and a slightly higher performance, with an increase in performance of 429% (with respect to J1) for J3s against 419% for J3r, making the square-based joint design J3s lighter and more performant than the round-based equivalent J3r. It suggests that square-based members are a slightly better choice than round-based members, which can be explained by their shape, allowing for a smaller (and therefore lighter) central joint piece while providing a larger surface of contact with the adhesive.

Manufacturing of the joints

The final aspect to take into consideration when choosing the most suited joint design for an application in trusses is the manufacturing of the joints. Considering only the joint designs J3s and J3r, as they were found to be much more performant than the joint designs J1, J2s and J2r, their differences in terms of manufacturing are the shape of the cross-section area of members, as it determines the shape of the holes that must be created into the central joint piece: full square for J3s; full round for J3r. Based on those shapes, the choice of the best joint design will depend on the type of manufacturing method that is available to the manufacturer.

- If only material-removal processes are available, full round holes can be achieved easily through mechanical drilling, while the other shapes would require more complex (and therefore most costly) processes, such as laser drilling. Further studies are required to find a good balance between performance and manufacturing cost, but the joint design J3r might be the best candidate if only material-removal processes are available to the manufacturer.
- If additive manufacturing processes are available to the manufacturer, more sophisticated shapes than a full round hole can be made easily. The selection of the best joint design can then be based on weight and performance only, since producing either shape for the central joint piece will not make a significant difference in the manufacturing cost. In this case, based on the discussion of the previous section, the joint design J3s is the best suited for an application in trusses. Following the same logic, more complex cross-sectional shapes, such as tubular sections, could provide even better performances. Further studies are required to find the best cross-sectional shape for this joint design.

It is to be noted that the materials for the adhesive and members are not taken into account in this discussion. The members being manufactured by pultrusion, producing either shape for their cross-section do not show a significantly different cost. However, the manufacturing considerations should also take into account the material used for the central joint piece, since not all materials are eligible for all manufacturing processes.

Conclusions

For an application in composite trusses and truss optimization, five joint designs were proposed. With the goal of comparing their performances in terms of strength and weight and selecting the one(s) that perform the best, numerical models were built in ABAQUS for each of the proposed designs. The models shared the same material properties, geometry, boundary conditions and element types, to reduce the influence of

those parameters of the joint performance as much as possible, and to focus the study on the joint design for the comparison of performances. Each model was analyzed in both the linear elastic domain and the non-linear domain, the latter taking into account the plasticity of the adhesive as well as non-linear geometry. The comparison of the performances of the models, based on the linear elastic analyses and the non-linear elastic analyses, showed that both types of analysis lead to slightly different conclusions.

Based on the results of the linear elastic analyses, it appeared that the joint design J3r, consisting in a central joint piece adhesively bonded to round-based members, showed the lowest peak shear strain value within the adhesive layer, suggesting that it is the strongest of the joint designs analyzed in this study. The results of the non-linear analyses lead to a different conclusion, with the joint design J3s, consisting in a central joint piece adhesively bonded to square-based members, showing the highest failure load. Relatively high discrepancies exist between the results of both analyses, with the non-linear analyses showing performances that are 1.6 times higher than those shown by the linear elastic analyses, suggesting that the linear models in their current state cannot predict these performances accurately enough. Taking into account the volume of the central joint piece in each of the joint designs, it appeared that, relatively to the least performant design, the increase in performance of each design does not always match the increase in weight of the joint piece volume. From the results of the linear elastic analyses, the joint designs J3s and J3r show the highest increase in performance relatively to the increase in volume, therefore we can consider them as being the most efficient of the joint designs analyzed in this study. From the results of the non-linear analyses, it appears that the joint design J3s performs better than the joint design J3r while also being lighter, which suggest that J3s is the most efficient one. Even though the performances and weights of the joint designs J3s and J3r are very close, their manufacturing requirements are different and favor J3r for being easier to manufacture if additive manufacturing is not available to the manufacturer.

Further numerical work, as well as experimental work, is needed to better understand and model the behavior of these promising joint designs. Obtaining a model that can predict the strength of a joint while being relatively low on computational cost would allow for an optimization of said joint designs, by varying parameters such as the overlap length or the amount of material in the central joint piece, to obtain a good balance between strength and low weight.

Authors' contributions
NPL is a Ph.D. Candidate at the Faculty of Aerospace Engineering of TU Delft, and the main author of this paper. OKB and DZ are the supervisors of the main author, providing counsel and assistance in the work done for this Ph.D. project. RB is the promotor of the Ph.D. project in which this work belongs. All authors read and approved the final manuscript.

Acknowledgements
Not applicable.

Competing interests
The authors declare that they have no competing interests.

Availability of data and materials
The data supporting the findings are presented in this manuscript.

Consent for publication
Not applicable.

Ethics approval and consent to participate
Not applicable.

Funding
This research is directly funded by the Faculty of Aerospace Engineering of TU Delft.

Publisher's Note

Received: 28 September 2017 Accepted: 6 December 2017
Published online: 13 December 2017

References

1. Michell AGM. The limits of economy of material in frame-structures. Philos Mag Ser. 1904;6(8):589–97. https://doi.org/10.1080/14786440409463229.
2. Dorn WS, Gomory RE, Greenberg HJ. Automatic design of optimal structures. J Mec. 1964;3:25–52.
3. Zegard T, Paulino GH. GRAND—ground structure based topology optimization for arbitrary 2D domains using MATLAB. Struct Multidiscip Optim. 2014;50:861–82. https://doi.org/10.1007/s00158-014-1085-z.
4. Zegard T, Paulino GH. GRAND3—ground structure based topology optimization for arbitrary 3D domains using MATLAB. Struct Multidiscip Optim. 2015;52:1161–84. https://doi.org/10.1007/s00158-015-1284-2.
5. Gao G, Liu Z, Li Y, Qiao Y. A new method to generate the ground structure in truss topology optimization. Eng Optim. 2016;273:1–17. https://doi.org/10.1080/0305215X.2016.1169050.
6. Zhang X, Maheshwari S, Ramos AS Jr, Paulino GH. Macroelement and macropatch approaches to structural topology optimization using the ground structure method. J Struct Eng. 2016;142:4016090. https://doi.org/10.1061/(ASCE)ST.1943-541X.0001524.
7. He L, Gilbert M. Rationalization of trusses generated via layout optimization. Struct Multidiscip Optim. 2015;52:677–94. https://doi.org/10.1007/s00158-015-1260-x.
8. Rajan SD. Sizing, shape, and topology design optimization of trusses using genetic algorithm. J Struct Eng. 1995;121:1480–7.
9. Deb K, Gulati S. Design of truss-structures for minimum weight using genetic algorithms. Finite Elem Anal Des. 2011;37:447–65.
10. Wu C-Y, Tseng K-Y. Truss structure optimization using adaptive multi-population differential evolution. Struct Multidiscip Optim. 2010;42:575–90. https://doi.org/10.1007/s00158-010-0507-9.
11. Lee KS, Geem ZW. A new structural optimization method based on the harmony search algorithm. Comput Struct. 2004;82:781–98. https://doi.org/10.1016/j.compstruc.2004.01.002.
12. Woods BKS, Hill I, Friswell MI. Ultra-efficient wound composite truss structures. Compos Part A Appl Sci Manuf. 2016;90:111–24. https://doi.org/10.1016/j.compositesa.2016.06.022.
13. Weaver TJ, Jensen DW. Mechanical characterization of a graphite/epoxy isotruss. J Aerosp Eng. 2000;13:23–35.
14. van den Berg LJ. Increasing the strength of an adhesive joint—MSc Thesis. Delft University of Technology. 2016.
15. Vallée T, Tannert T, Hehl S. Experimental and numerical investigations on full-scale adhesively bonded timber trusses. Mater Struct. 2011;44:1745–58. https://doi.org/10.1617/s11527-011-9735-8.
16. Volkersen O. Die Nietkraftverteilung in zugbeanspruchten Nietverbindungen mit konstanten Laschenquerschnitten. Luftfahrtforschung. 1938;15:41–7.
17. Goland M, Reissner E. The stresses in cemented joints. J Appl Mech. 1944;11:A17–27.
18. Bigwood DA, Crocombe AD. Elastic analysis and engineering design formulae for bonded joints. Int J Adhes Adhes. 1989;9:229–42. https://doi.org/10.1016/0143-7496(89)90066-3.
19. Gonçalves J, de Moura M, de Castro P. A three-dimensional finite element model for stress analysis of adhesive joints. Int J Adhes Adhes. 2002;22:357–65. https://doi.org/10.1016/S0143-7496(02)00015-5.
20. Adams RD, Peppiatt NA. Stress analysis of adhesive-bonded lap joints. J Strain Anal Eng Des. 1974;9:185–96. https://doi.org/10.1243/03093247V093185.
21. Grant LDR, Adams RD, da Silva LFM. Experimental and numerical analysis of single-lap joints for the automotive industry. Int J Adhes Adhes. 2009;29:405–13. https://doi.org/10.1016/j.ijadhadh.2008.09.001.
22. Broughton RW, Crocker LE, Urquhart JM. Strength of adhesive joints: a parametric study. 2001. https://doi.org/10.1038/2021087a0.
23. Banea MD, da Silva LFM, Carbas R, Campilho RDSG. Effect of material on the mechanical behaviour of adhesive joints for the automotive industry. J Adhes Sci Technol. 2016;4243:1–14. https://doi.org/10.1080/01694243.2016.1229842.
24. Fernandes TAB, Campilho RDSG, Banea MD, da Silva LFM. Adhesive selection for single lap bonded joints: experimentation and advanced techniques for strength prediction. J Adhes. 2015;91:841–62. https://doi.org/10.1080/00218464.2014.994703.
25. ZOLTEK Carbon Fiber ZOLTEK PX35—Standard fiber properties. http://zoltek.com/products/panex-35/. Accessed 31 May 2017.
26. HEXION Inc. EPIKOTE Resin MGS LR285—technical data sheet. http://www.hexion.com/Products/TechnicalDataSheet.aspx?id=30303. Accessed 31 May 2017.
27. Huntsman Advanced Materials Inc. Araldite 2015 Adhesive. 2015. https://us.aralditeadhesives.com/index.php?option=com_docman&view=download&alias=166-araldite-2015-us-e&Itemid=146&lang=us. Accessed 11 Dec 2017.
28. Campilho RDSG, Pinto AMG, Banea MD, et al. Strength improvement of adhesively-bonded joints using a reverse-bent geometry. J Adhes Sci Technol. 2011;25:2351–68. https://doi.org/10.1163/016942411X580081.

29. Bagheri R, Marouf BT, Pearson RA. Rubber-toughened epoxies: a critical review. Polym Rev. 2009;49:201–25. https://doi.org/10.1080/15583720903048227.
30. ASM Aerospace Specification Metals Inc. Aluminum 7075-T6 Datasheet. http://asm.matweb.com/search/SpecificMaterial.asp?bassnum=MA7075T6. Accessed 9 June 2017.
31. Díaz J, Romera L, Hernández S, Baldomir A. Benchmarking of three-dimensional finite element models of CFRP single-lap bonded joints. Int J Adhes Adhes. 2010;30:178–89. https://doi.org/10.1016/j.ijadhadh.2009.12.005.
32. Dassault Systemes ABAQUS 2016 documentation. http://50.16.225.63/v2016/. Accessed 25 Aug 2017.
33. Harris JA, Adams RA. Strength prediction of bonded single lap joints by non-linear finite element methods. Int J Adhes Adhes. 1984;4:65–78. https://doi.org/10.1016/0143-7496(84)90103-9.
34. Campilho RDSG, Banea MD, Neto JABP, Da Silva LFM. Modelling adhesive joints with cohesive zone models: effect of the cohesive law shape of the adhesive layer. Int J Adhes Adhes. 2013;44:48–56. https://doi.org/10.1016/j.ijadhadh.2013.02.006.
35. Campilho RDSG, Banea MD, Neto JABP, da Silva LFM. Modelling of single-lap joints using cohesive zone models: effect of the cohesive parameters on the output of the simulations. J Adhes. 2012;88:513–33. https://doi.org/10.1080/00218464.2012.660834.